HEFAT2012
9th International Conference on Heat Transfer, Fluid Mechanics and Thermodynamics
16 – 18 July 2012
Malta

INFLUENCE OF THE GEOMETRY ON THE THERMOHYDRAULICS OF A COMPOUND HEAT EXCHANGER CONSISTING OF LOUVERED FINS AND DELTA WINGLETS

Huisseune H.[1,*], T'Joen C.[1], De Jaeger P.[1,2], Ameel B.[1], De Schampheleire S.[1] and De Paepe M.[1]
*Author for correspondence
[1]Ghent University, Department of Flow, Heat and Combustion Mechanics,
Sint-Pietersnieuwstraat 41, 9000 Gent, Belgium
[2]NV Bekaert SA, Bekaertstraat 2, 8550 Zwevegem, Belgium
E -mail: Henk.Huisseune@UGent.be

ABSTRACT

Louvered fin heat exchangers with round tubes are frequently used in heating, ventilation, air conditioning and refrigeration applications. In this paper delta winglet vortex generators are punched out of the louver surface, resulting in a so called compound design. Three-dimensional numerical simulations were performed. The delta winglets serve to reduce the size of the tube wakes, which are zones of poor heat transfer. A screening analysis of the most important geometrical parameters showed that the delta winglet geometry highly contributes to the thermal and hydraulic performance at low Reynolds numbers, while at higher Reynolds numbers the performance is mainly determined by the louver geometry. The compound heat exchanger has a better thermal hydraulic performance than when the louvers or the delta winglets are applied separately. The performance of the compound design is also compared to louvered, slit and plain fin heat exchangers. This clearly shows its potential. Especially for low Reynolds applications, the compound heat exchanger can be made smaller in size and thus more economical in cost.

INTRODUCTION

Every day large amounts of heat are transferred in many industrial and domestic processes using heat exchangers. Any energy savings in the heat transfer process have a significant impact on the fuel consumption and the greenhouse gas emissions. In many applications air is one of the working fluids (e.g. coolers in compressed air systems, heat pumps, air conditioning devices, domestic heating, etc.). In these low Reynolds applications, the main thermal resistance is located at the air side of the heat exchanger. To increase the heat transfer rate, the heat transfer surface area is enlarged by adding fins to the air side. When a high compactness is desired, complex interrupted fin patterns are used. A typical example is the louvered fin design, as shown in Figure 1a. This design consists of an array of flat plates (louvers) set at an angle to the incoming flow. The geometrical parameters are also indicated in Figure 1a. The interrupted section of Figure 1a needs to be connected to the tubes to form the heat exchanger.

Through a finite-difference analysis, Achaichia and Cowell [1] showed that increasing the Reynolds number results in a transition in the flow behavior from duct-directed to more louver-directed flow (see Figure 1b). At low Reynolds numbers the thick boundary layers block the passage between the louvers, forcing the flow to go straight through. As the Reynolds number increases, the boundary layers become thinner and the passage opens up, aligning the flow with the louvers and extending the flow path. This results in an increased heat transfer rate. But as the flow path is extended, the frictional pressure drop also increases. The degree to which the flow follows the louvers is quantified by the flow efficiency, which is defined as the ratio of the mean flow angle to the louver angle [2]. Next to the Reynolds number, the flow efficiency is also strongly dependent on the louvered geometry. This is shown by Zhang and Tafti [2] through numerical simulations. These numerical findings agree well with the flow visualization experiments of DeJong and Jacobi [3].

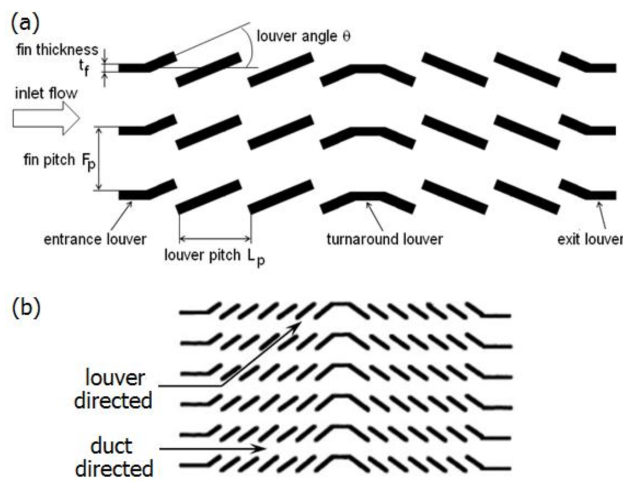

Figure 1 (a) Louver array with geometrical parameters; (b) Duct vs. louver-directed flow

The main disadvantage of the louvered fins is the high pressure drop. Vortex generators mounted on a heat transfer surface generate vortices which cause an intense mixing of the flow and thin the thermal boundary layers. In contrast to louvered fins, they enhance the heat transfer with a relatively low penalty in pressure drop. A typical example are delta winglets, see Figure 2a. When delta winglets are used in fin and tube heat exchangers, they can reduce the poor heat transfer region in the tube wakes. A common flow down configuration, as presented in Figure 2b, is frequently used. The delta winglet pair is placed downstream the tube in the near wake region in order to introduce high momentum fluid behind the tube and improve the poor heat transfer in the wake region [4].

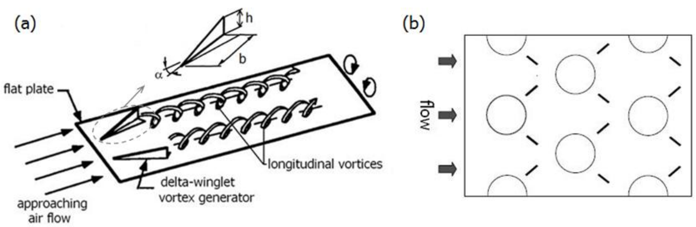

Figure 2 (a) Delta winglet pair on a flat plate generating longitudinal vortices [5]; (b) Common flow down orientation of winglet pairs on the fin of a round tube heat exchanger [6].

Heat exchanger manufacturers are continuously searching for new and better designs. As suggested by Bergles [7], the next generation of heat exchangers will combine existing enhancement techniques. This results in so called compound designs. Examples are the combination of wavy fins and vortex generators [8-9] or offset strip fins and vortex generators [10-11]. To the authors' knowledge, only a few studies on compound designs with louvered fins and vortex generators can be found in literature. Joardar and Jacobi [12] tested a louvered fin heat exchanger with flat tubes before and after adding leading edge delta wings on the heat exchanger face. By adding delta wings the average heat transfer enhancement was 21% under dry conditions and 23.4% under wet surface conditions for inlet velocities between 1 and 2 m/s. The associated pressure drop penalty was about 6%. Joardar and Jacobi [12] believe that further improvements are possible by optimizing the wing geometry and placement. Lawson and Thole [13] stamped delta winglets into the flat landings between the louvers and flat tube of a heat exchanger and they evaluated the tube wall heat transfer augmentation and associated pressure drop. They found an enhancement in tube wall heat transfer up to 47% with a corresponding pressure drop penalty of 19%.

The studies on compound heat exchangers with louvers and vortex generators focus on flat tube heat exchangers. In this work delta winglets are added to the louvered fins of a heat exchanger with round tubes. The flow structures which affect the heat transfer and pressure drop were previously discussed by Huisseune et al. [14]. In this paper a screening analysis is performed of the most important geometrical parameters using Computational Fluid Dynamics (CFD). The performance of the compound heat exchanger is also compared to the performance of existing enhanced heat exchangers.

NOMENCLATURE

A_c	[m²]	Minimum cross sectional flow area
A_o	[m²]	External heat transfer surface area
A_f	[m²]	Fin surface area
b	[m]	Delta winglet base
c_p	[J/kgK]	Specific heat capacity
D_h	[m]	Hydraulic diameter (Eq. (7))
D_o	[m]	Outer tube diameter
f	[-]	Friction factor (Eq. (6))
F_n	[-]	Pumping power factor according to Soland et al. [15] (Eq. (9))
F_p	[m]	Fin pitch
G_c	[kg/m²s]	Mass flux in the minimum cross sectional flow area
h	[m]	Delta winglet height
h^*	[-]	Height ratio of the delta winglet
h_o	[W/m²K]	External convection coefficient
j	[-]	Colburn j-factor (Eq. (5))
J_n	[-]	Heat transfer performance factor according to Soland et al. [15] (Eq. (8))
L	[m]	Flow depth
L_p	[m]	Louver pitch
$\dot{m}$	[kg/s]	Mass flow rate
ΔP	[Pa]	Pressure drop
Pr	[-]	Prandtl number
Q	[W]	Heat transfer rate
Re_{Dh}	[-]	Reynolds number based on the hydraulic diameter and the velocity in the minimal cross sectional flow area
s	[m]	Fin spacing = difference between fin pitch and fin thickness
T	[K]	Temperature
t_f	[m]	Fin thickness
V_c	[m/s]	Velocity in the minimal cross sectional flow area
P_l	[m]	Longitudinal tube pitch
P_t	[m]	Transversal tube pitch
Δx	[m]	Streamwise delta winglet position
Δz	[m]	Spanwise delta winglet position

Greek symbols

α	[°]	Angle of attack of the delta winglet vortex generator
η_o	[-]	Surface efficiency
η_f	[-]	Fin efficiency
λ	[W/mK]	Thermal conductivity
Λ	[-]	Delta winglet aspect ratio (= b/h)
ν	[m²/s]	Kinematic viscosity
θ	[°]	Louver angle
ρ	[kg/m³]	density
σ	[-]	Contraction ratio (i.e. the ratio of the minimal cross sectional flow area to the frontal area)

THREE-DIMENSIONAL COMPUTATIONAL DOMAIN

The three-dimensional computational domain of the louvered fin geometry with vortex generators is shown in Figure 3. Three tube rows in a staggered arrangement are considered. Delta winglet vortex generators are punched out of the fin surface in a common flow down arrangement behind each tube. Each louver element between the tubes consists of an inlet louver, an exit louver and two louvers on either side of the turnaround louver. Each louver transitions from an angle θ into a flat landing adjoining the tube surface. The spanwise dimensions of the flat landing and transition part were chosen as in [16-17], i.e. $0.25L_p$ for the minimum flat landing (between the turnaround louver and tube) and $0.5L_p$ for the transition part. Periodic conditions are applied on both sides of the domain as well as on the top and bottom. The height of the computational domain is equal to the fin pitch F_p and the width is equal to transversal tube pitch P_t. The geometry is located in the middle with half a fin spacing above the fin surface and half a fin spacing below. The entrance length upstream of the fin equals 5 times the fin pitch F_p and the domain extends 7 times the tube diameter D_o downstream of the fin, as was suggested by Jang et al. [18].

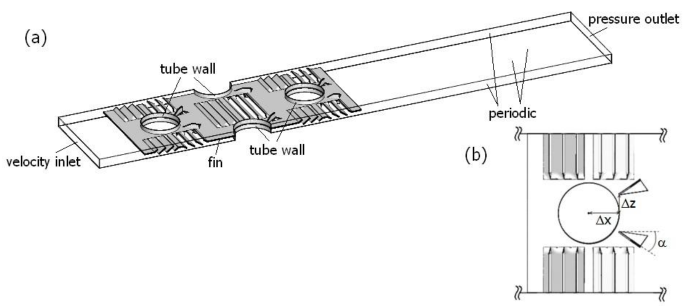

Figure 3 (a) three-dimensional computational domain and (b) top view showing the delta winglet position

COMPUTATONAL METHOD

The mesh was generated using Gambit©. The solid fin material as well as the air domain were meshed to take fin conduction into account. The quality of the mesh was carefully assessed during the meshing. The computational domain was divided into several subdomains. The fin material was meshed with quad elements. Most of the air subdomains were also meshed with quad elements. Only the subdomains with the transition zone between the angled louver and flat landing and the subdomains surrounding the delta winglets were meshed using unstructured tetrahedral elements. The cell size gets smaller towards the fin surface to capture velocity and temperature gradients.

The commercial code ANSYS Fluent© 12.0.16 is used for the simulations. The flow is assumed to be laminar, which is acceptable in the considered Reynolds range (Re_{Dh} = 100 – 1400) [19]. At the inlet a uniform velocity parallel to the fin was imposed and the air temperature was set to 293K. At the outlet the static pressure was set to 0 Pa (pressure outlet boundary condition). A constant tube wall temperature of 323K was applied in the three tube rows. No slip boundary conditions were applied on the tube and fin surfaces. The double precision segregated solver was used to solve the standard Navier-Stokes equations. The energy equation was turned on to compute the heat transfer through the tube walls and fin material and in the air. The SIMPLE algorithm was applied for the pressure-velocity coupling. The discretization of the convective terms in the governing equations was done via a second order upwind scheme, while a second order central differencing scheme was applied for the diffusive terms. The gradients were evaluated via the least squares cell based method. The pressure gradient in the momentum equations was treated via a second order discretization scheme. Convergence criteria were set to 10^{-8} for continuity, velocity components and energy. Setting smaller values for these criteria did not result in any notable differences in the flow field and heat transfer predictions. The air density was calculated as for an incompressible ideal gas, the specific heat and thermal conductivity were set to constant values (c_p = 1006 J/kgK; λ = 0.02637 W/mK) and the dynamic viscosity was calculated with the Sutherland approximation. The fin has a thermal conductivity of 202.4 W/mK.

Only for the smallest Reynolds numbers (Re_{Dh} < 200) steady simulations were found to converge. For higher Reynolds numbers unsteady simulations were performed (first order accurate in time). The time step varied between 1 μs and 1 ms (dependent on the Reynolds number). This allowed the residuals to decrease below 10^{-8} in less than 50 iterations per time step. The mass-weighted average pressure drop and outlet temperature were monitored during the iterations to determine if the simulations had converged. Local temperatures in the tube and louver wakes were also monitored. Once convergence was reached, these temperatures varied in function of the time around a mean value. The data of the unsteady simulations reported in this paper are the time averaged values. They were averaged out over the time interval an air particle needs to travel about three times the length of the computational domain. Averaging over a longer time interval did not result in any notable differences. For each simulation the energy balance was checked: the net heat transfer rate between the air inlet and outlet differs less than 0.01% from the total heat transfer rate of the tube and fin surface.

DATA REDUCTION METHOD

The heat transfer rate Q at the air side was determined as:

$$Q = m_{air}\bar{c}_{p,air}\left(T_{air,out} - T_{air,in}\right) \tag{1}$$

with $\bar{c}_p$ the mean specific heat capacity between the inlet and outlet temperatures. The air side convection coefficient was calculated using the LMTD (logarithmic mean temperature difference) method:

$$h_o = \frac{Q}{\eta_o A_o F\ LMTD} \tag{2}$$

A_o is the total exterior heat transfer surface area and η_o is the surface efficiency. Due to the fixed wall temperature the correction factor F is equal to unity [20]. The logarithmic mean temperature difference is expressed as:

$$LMTD = \frac{\left(T_{wall} - T_{air,out}\right) - \left(T_{wall} - T_{air,in}\right)}{ln\left(\frac{T_{wall} - T_{air,out}}{T_{wall} - T_{air,in}}\right)} \tag{3}$$

The surface efficiency η_o was calculated with the fin efficiency η_f:

$$\eta_o = 1 - \frac{A_f}{A_o}\left(1 - \eta_f\right) \quad (4)$$

A_f is the fin surface. The fin efficiency η_f is obtained using the equivalent circular fin method of Schmidt [21], which is also used by many other authors [22-24]. Because the fin efficiency is dependent on the air side convection coefficient h_o, it resulted from iterative calculations. The air side convection coefficient is represented dimensionless as the Colburn j-factor:

$$j = \frac{h_o}{\rho \cdot c_p \cdot V_c} \cdot Pr^{2/3} \quad (5)$$

V_c is the velocity in the minimum cross sectional flow area and Pr is the Prandtl number. The pressure drop across the heat exchanger is presented as the fanning friction factor. This friction factor is calculated as proposed by Kays and London [25]:

$$f = \frac{A_c}{A_o}\frac{\rho_m}{\rho_{in}}\left[\frac{2\rho_{in}\Delta P}{G_c^2} - \left(1+\sigma^2\right)\left(\frac{\rho_{in}}{\rho_{out}} - 1\right)\right] \quad (6)$$

G_c is the mass flux in the minimal cross sectional flow area A_c. The contraction ratio σ is defined as the ratio of A_c to the frontal area. The friction factor includes the entrance and exit pressure loss.

VALIDATION OF THE NUMERICAL RESULTS

A grid independency study showed that the simulations are grid independent. Also a validation experiment in a wind tunnel was performed. There is a good match between the numerical results and the experimental measurements within the experimental uncertainty: the difference between the numerical and experimental Colburn j-factors is on average 6.2% and the difference between the numerical and experimental friction factors is on average 5.5%. More details can be found in Huisseune [26] (not shown here due to space restrictions).

GEOMETRICAL DETAILS

Many geometrical parameters have an influence on the thermal hydraulic performance of the compound design. Some of these parameters have a small impact, others have a larger impact. If only one factor is varied at a time (the so called full factorial analysis), a very large number of cases has to be simulated if more than three parameters are considered. This is very time and resource consuming. However, Taguchi [27] suggested the use of orthogonal arrays, which significantly reduces the number of simulations. Orthogonal arrays only identify the main effects, but not the interactions between the geometrical parameters (also called control parameters or design variables). This allows for a time efficient screening of a large number of parameters. The Taguchi method [27] allows determining which control parameters have a higher impact on the performance. Hence, it indicates with a limited number of simulations which parameters are most important for optimization. This method was already used for heat exchanger optimization by Qi et al. [28], Sahin [29] and Zeng et al. [30].

Selection of the control parameters

The louver pitch and louver angle significantly influence the thermal hydraulic performance of louvered fin heat exchangers [28, 31-32]. These parameters most probably also have an important impact on the performance of compound designs and thus they are considered as two of the control parameters during the Taguchi analysis. The delta winglet geometry is determined by the angle of attack α, the delta winglet height h, the delta winglet aspect ratio Λ and the delta winglet position. The delta winglet aspect ratio Λ is defined as the ratio of the delta winglet base b to the delta winglet height h. Pesteei et al. [33] studied the optimal position of a delta winglet pair in common flow down configuration and they found that $\Delta x = 0.5D_o$ and $\Delta z = \pm 0.5D_o$ resulted in the best heat transfer to pressure drop performance (D_o is the outer tube diameter and Δx and Δz are respectively the streamwise and spanwise distance between the tube center and the point where the leading edge of the winglet intersects with the fin surface, as indicated in Figure 3b). In the compound design Δz has to be smaller than $0.5D_o$ due to the presence of the louvers (for $\Delta z = 0.5D_o$ no angle of attack is possible for the delta winglet in common flow down orientation). A fixed vortex generator position of $\Delta x = 0.5D_o$ and $\Delta z = \pm 0.3D_o$ was selected which allows a maximum angle of attack of 35°. The angle of attack α, delta winglet height h and delta winglet aspect ratio Λ are considered as control parameters.

Three levels are assigned to each of the five control parameters. Table 1 lists the control parameters and their levels. The delta winglet height h is made dimensionless with the fin spacing ($h^* = h/s$). The levels are selected based on a literature review. The database of Wang et al. [22] contains samples with a fin pitch ranging from 1.20 to 1.99 mm for louvered fin heat exchangers similar to the geometry tested in this study. The three fin pitches were chosen in this range. The louver angle in louvered fin heat exchangers typically lies between 14° and 35° [34]. Here, louver angles of 22°, 28° and 35° were selected. Fiebig et al. [35] showed that for a plain fin heat exchanger the highest heat transfer coefficients on the fin are obtained for a delta winglet pair with an angle of attack α = 45°. Due to the presence of the louvers, the delta winglet angle in the compound design is smaller than 45°. The three angles of attack used in the Taguchi analysis are 25°, 30° and 35°. The delta winglet height used by Fiebig et al. [35] was half of the channel height. A delta winglet height equal to 90% of the channel height is also frequently used [6, 36-38]. The third level of the delta winglet height was set in between these two levels, i.e. 70% of the channel height. The three aspect ratio levels used in the simulations are 1.0 [35], 1.5 [33] and 2.0 [6,36,39].

Table 1 Levels of each control parameter (DW = delta winglet)

Control parameter	Symbol	Level 1	Level 2	Level 3
Fin pitch	F_p (mm)	1.20	1.71	1.99
Louver angle	θ (°)	22	28	35
DW angle of attack	α (°)	35	30	25
DW height ratio	h*	0.9	0.7	0.5
DW aspect ratio	Λ	1.0	1.5	2.0

Orthogonal array

For a full factorial analysis 243 (= 3^5) simulations are required. This number can be reduced by selecting an appropriate orthogonal array. The orthogonal array L9 (3^5) developed by Bolboaca and Jäntschi [40] is used in this study, see Table 2. Nine geometries are simulated to test the influence of the five control parameters. For each of these five factors, three geometries need to be simulated per level, which is a characteristic of the orthogonal matrix. The remaining geometrical parameters are fixed during the simulations. Their values were selected based on the database of Wang et al. [22] for louvered fin heat exchangers. They are listed in Table 3. The effect of the inlet velocity on the thermal hydraulic performance of heat exchangers is obvious. That is why the velocity is not considered as a control parameter, but each of the nine geometries is simulated for two different inlet velocities (V_{in} = 0.63 m/s and 5.25 m/s). A commonly used criterion to evaluate the thermal hydraulic performance of a heat exchanger is the area goodness factor. It is defined as the ratio of the Colburn j-factor to the friction factor. High values of j/f are preferred as this means less frontal area for a fixed heat transfer and pressure drop [41]. The effect of the five control parameters on the area goodness factor is evaluated for both inlet velocities individually.

Table 2 Orthogonal array L9 (3^5) used for Taguchi analysis (from [40])

no.	F_p (mm)	θ (°)	α (°)	h*	Λ
1	1.20	22	35	0.9	1.0
2	1.20	22	25	0.5	1.5
3	1.20	35	35	0.5	2.0
4	1.71	28	25	0.9	2.0
5	1.71	35	30	0.9	1.5
6	1.71	35	25	0.7	1.0
7	1.99	22	30	0.7	2.0
8	1.99	28	35	0.7	1.5
9	1.99	28	30	0.5	1.0

Table 3 Geometrical parameters fixed during Taguchi analysis

Parameter	Symbol	Value
Outer tube diameter	D_o (mm)	6.75
Fin thickness	t_f (mm)	0.12
Louver pitch	L_p (mm)	1.5
Transversal tube pitch	P_t (mm)	17.6
Longitudinal tube pitch	P_l (mm)	13.6
Streamwise DW position	Δx (mm)	$0.5D_o$
Spanwise DW position	Δz (mm)	$0.3D_o$

RESULTS AND DISCUSSION

Screening analysis

The contribution ratios of each control parameter are calculated in a similar way as by Qi et al. [28] for louvered fin heat exchangers and by Zeng et al. [30] for plain fin heat exchangers with vortex generators. The calculated area goodness factors for the nine simulation cases at an inlet velocity of 0.63 m/s are shown in Table 4. The factorial effect and contribution ratio of each control parameter are presented in Table 5 and Figure 4a. The area goodness factor of each control parameter in Table 5 is the arithmetic mean of the area goodness factors corresponding to each level in Table 4. R is the difference between the minimum and maximum averaged area goodness factor for each control parameter. The contribution ratio equals the value R of each control parameter divided by the total R of all control parameters. The contribution ratio thus indicates the influence of each control parameter on the area goodness factor. The calculations for V_{in} = 5.25 m/s are similar. Due to space restrictions, these results are only shown graphically (see Figure 4b).

Table 4 Area goodness factor for each simulation case at V_{in} = 0.63 m/s

no.	F_p (mm)	θ (°)	α (°)	h*	Λ	j/f
1	1.20	22	35	0.9	1.0	0.2055
2	1.20	22	25	0.5	1.5	0.2080
3	1.20	35	35	0.5	2.0	0.1843
4	1.71	28	25	0.9	2.0	0.2751
5	1.71	35	30	0.9	1.5	0.2501
6	1.71	35	25	0.7	1.0	0.2527
7	1.99	22	30	0.7	2.0	0.2871
8	1.99	28	35	0.7	1.5	0.2944
9	1.99	28	30	0.5	1.0	0.2978

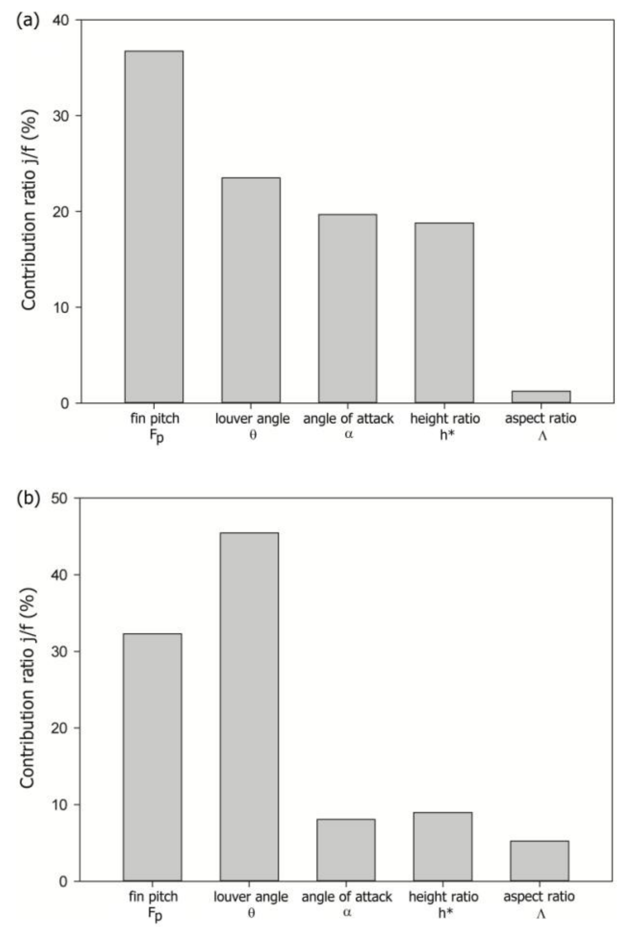

Figure 4 Contribution ratio to the area goodness factor of each control parameter: (a) V_{in} = 0.63 m/s and (b) V_{in} = 5.25 m/s

Table 5 Factorial effect on and contribution ratio to the area goodness factor for each control parameter at V_{in} = 0.63 m/s

	Level	F_p (mm)	θ (°)	α (°)	h*	Λ
Area goodness factor	1	0.1993	0.2336	0.2281	0.2436	0.2520
	2	0.2593	0.2891	0.2783	0.2781	0.2508
	3	0.2931	0.2290	0.2453	0.2300	0.2488
R (max – min)	0.255	0.0938	0.0600	0.0502	0.0480	0.0032
Contribution ratio (%)	100	36.7	23.5	19.7	18.8	1.2

Figure 4 illustrates the clear difference between the low and high velocity. For the highest velocity (V_{in} = 5.25 m/s, Figure 4b) the louver angle provides the main contribution to the area goodness factor (about 46%), followed by the fin pitch (around 32%). The influence of the delta winglet geometry is much smaller: the winglet parameters contribute less than 10% to the area goodness factor. For the lowest velocity (V_{in} = 0.63 m/s, Figure 4a) the main contribution is provided by the fin pitch (37%). But for this low velocity also the angle of attack and height ratio of the delta winglets are important design parameters. Their contribution is of the same order as the contribution of the louver angle (about 20%). The effect of the delta winglet aspect ratio is negligible. The difference in contribution to the thermal hydraulic performance of the low and high velocities is related to the difference in the flow field. At low air velocities the flow passage between the louvers is blocked by the thick boundary layers and thus the flow efficiency is low. The flow is more duct directed and thus the longitudinal vortices generated by the delta winglets are not immediately destroyed by the deflected flow when entering the downstream tube row, as explained in Huisseune et al. [14]. Also the wake zones behind the tubes are large and stable. Hence the reduction of these wake zones by the delta winglets has a large contribution to the thermal hydraulic performance. At high velocities, however, the flow is more louver directed. The longitudinal vortices do not propagate far downstream in the heat exchanger as they are destroyed by the deflected flow when entering the downstream tube row. The wake zones are also less stable and thus the influence of the delta winglet geometry is relatively seen smaller. Thus at high velocities the louvers dominate the thermal hydraulic performance, while at low velocities also the delta winglet geometry plays an important role.

Comparison with other enhanced fin designs

To illustrate the potential of the compound heat exchanger, its performance is compared to the performance of slit fin and louvered fin designs. These are the most widely used interrupted fin surfaces. Also plain fins are considered for comparison. Their Colburn and friction characteristics are determined with correlations found in literature (louvered fins [22], slit fins [42] and plain fins [43]). These three literature correlations are developed by the same research group and the data reduction method is identical to the method used in this work.

The details of the compound heat exchanger which is considered for comparison are listed in Table 6. For this geometry, the heat transfer and pressure drop of heat exchangers in which the individual enhancement techniques are applied separately (thus only delta winglets or only louvers) are also simulated. The resulting louvered fin heat exchanger differs from the louvered fin heat exchangers covered by the literature correlation [22] as the latter have X shaped louvers surrounding the tubes (in contrast to the rectangular louver design used in the simulations). This difference is illustrated in Figure 5. The X shapes have more louvered fin surface per unit heat transfer surface area and they cause a better mixing in the tube wakes. However, they prevent the formation of horseshoe vortices and they also cause a higher pressure drop. The literature correlations can only be used within the geometry ranges of the experimental data they are based on. Outside these ranges no reliable predictions can be made. Hence, the geometries used to evaluate the literature correlations were chosen within their applicability ranges. To make a fair comparison heat exchangers with the same heat transfer surface A_o are studied. A same heat transfer surface means that the material cost of the heat exchangers is the same. The dimensions of the heat exchangers are listed in Table 7. The number of tube rows and the longitudinal tube pitch are chosen the same as for the compound design (N = 3 and P_l = 13.6 mm). The transversal tube pitch P_t of the louvered, slit and plain fin heat exchangers is then changed until the heat transfer surface A_o is identical to the heat transfer surface of the compound design. The values are within the applicability range of the corresponding correlations. The values of the other geometrical parameters are the dimensions of a heat exchanger with a tube diameter as close as possible to the simulated D_o = 6.75 mm. These are selected from the database which was used to fit the correlations [22,42-43]. The louvered fin heat exchanger selected from the database of Wang et al. [22] has the same number of louvers per louver array as the simulated compound heat exchanger and the louvered only heat exchanger: an inlet louver, an exit louver and two louvers on either side of the turnaround louver.

Table 6 Compound heat exchanger used in comparison study

Parameter	**Symbol**	**Value**
Outer tube diameter	D_o (mm)	6.75
Fin thickness	t_f (mm)	0.12
Louver pitch	L_p (mm)	1.5
Louver angle	θ (°)	35
Fin pitch	F_p (mm)	1.71
Transversal tube pitch	P_t (mm)	17.6
Longitudinal tube pitch	P_l (mm)	13.6
Streamwise DW position	Δx (mm)	$0.5D_o$
Spanwise DW position	Δz (mm)	$0.3D_o$
DW Angle of attack	α (°)	35
DW height ratio	h*	0.9
DW aspect ratio	Λ	2

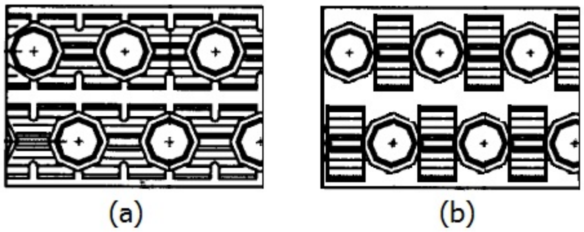

Figure 5 (a) X-shaped louver layouts around the tubes [22] and (b) rectangular shaped louver layouts between the tubes

Table 7 Heat exchanger dimensions used in the comparison study: the heat transfer surface Ao is fixed (by changing Pt and N = 3, Pl = 13.6 mm) and the other dimensions are selected from the respective databases [22,42-43]

Parameter	**Symbol**	**Louvers [22]**	**Slits [42]**	**Plain [43]**
Outer tube diameter	D_o (mm)	6.7	7.3	6.7
Transversal tube pitch	P_t (mm)	17.5	18.2	17.5
Longitudinal tube pitch	P_l (mm)	13.6	13.6	13.6
Fin pitch	F_p (mm)	1.98	1.6	1.98
Fin thickness	t_f (mm)	0.115	0.11	0.115
Number of tube rows	N	3	3	3
slit height	S_h (mm)		1.6	
slit breadth	S_s (mm)		1	
number of slits	S_n		7	
louver height	L_h (mm)	1.4		
louver angle	θ (°)	39		

The performance of the heat exchangers is evaluated based on the Colburn j-factor and the friction factor. They are plotted as function of the Reynolds number Re_{Dh} which is based on the velocity V_c in the minimum cross sectional flow area and the hydraulic diameter D_h:

$$D_h = \frac{4A_cL}{A_o} \tag{7}$$

with A_c the minimum cross sectional flow area, L the flow depth and A_o the total heat transfer surface area. Soland et al. [15] suggested evaluating the thermal hydraulic performance of heat exchangers by plotting the heat transfer performance factor J_n (Eq. (8)) as function of the pumping power factor F_n (Eq. (9)). J_n is proportional to the heat transfer per unit volume and F_n is proportional to the pumping power per unit volume. J_n vs. F_n is thus a modification of the volume goodness factor proposed by London and Ferguson [44]. Also this performance evaluation criterion is used here as it allows a comparison in terms of total heat transfer surface area or core volume.

$$J_n = \sigma \cdot \frac{j \cdot Re_{Dh}}{D_h^2} \tag{8}$$

$$F_n = \sigma \cdot \frac{f \cdot Re_{Dh}^3}{D_h^4} \tag{9}$$

The results are plotted in Figure 6. The symbols represent simulated data of the compound heat exchanger, the heat exchanger with only louvers and the heat exchanger with only delta winglets. The Colburn j-factors of the compound design are higher than when the individual enhancement techniques are applied separately (up to 16% higher compared to the louvered fin heat exchanger and up to 87% higher compared to the delta winglet heat exchanger). Also the associated friction factors are higher (up to 37% higher compared to the louvered fin heat exchanger and up to 156% higher compared to the delta winglet heat exchanger). If heat transfer as well as pressure drop are considered in terms of the modified volume goodness factor, then the compound design outperforms the simulated louvered fin heat exchanger and delta winglet heat exchanger. For a fixed pumping power per unit volume, the heat transfer per unit volume of the compound design is up to 14% higher compared to the louvered fin heat exchanger and up to 72% higher compared to the delta winglet heat exchanger. For the same thermal hydraulic performance, the compound heat exchanger can thus be made smaller in size. As a result, the material cost is lower and also the operational cost (pumping power) is (often) reduced.

The full lines in Figure 6 correspond to the literature correlations of the louvered fin heat exchanger, the slit fin heat exchanger and the plain fin heat exchanger of Table 7. The louvered fin and slit fin correlations consist of two parts depending on the Reynolds number. This explains the discontinuity in the curves. The plain fin heat exchanger shows the lowest Colburn j-factor, friction factor and volume goodness. This heat exchanger is only used if a low pressure drop is demanded and volume is not an issue. If a high compactness is needed, interrupted fin surfaces are used.

From a thermal point of view, the compound design clearly shows advantage at low Reynolds numbers: the Colburn j-factors are higher. As explained before, at low Reynolds numbers the delta winglets highly contribute to the thermal performance. The associated friction factors are also higher. The volume goodness plot indicates that for the same pumping power and heat transfer surface, the compound design yields a higher heat transfer performance. Thus for the same material cost and pumping power cost, the compound design has a better cooling or heating capacity.

The discontinuity in the louvered fin Colburn correlation appears for Re_{Dc} = 1000 (Reynolds number based on the collar diameter D_c and the velocity in the minimum cross section flow area V_c). This corresponds for the given geometry with an inlet velocity of about 1.4 m/s. Thus for low Reynolds applications, such as HVAC&R, the combination of louvered fins and delta winglets clearly shows potential. For domestic air conditioning devices, for instance, the inlet velocity is typically 1.3 m/s [45]. When using a compound design instead of a louvered fin heat exchanger the heat exchanger can be smaller in volume for the same heat duty. The associated pumping power is then also lower. Alternatively, for the same heat exchanger volume, the compound design can work at lower velocities. This is interesting for air conditioning applications with a unit installed in the room, because then low velocities are preferred: a high velocity air jet blown into the room feels uncomfortable for the room occupants and lower velocities also cause less noise.

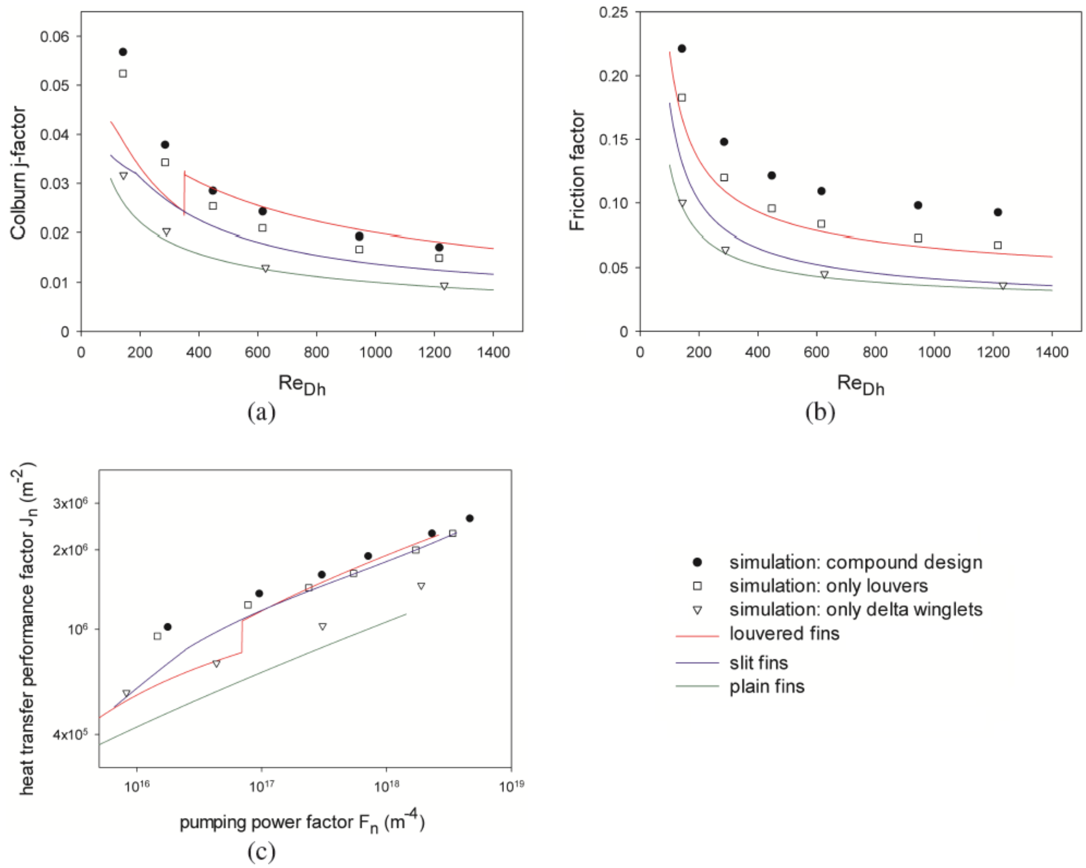

Figure 6 Comparison of the simulation data with louvered fins [22], slit fins [42] and plain fins [43] (fixed A_o): (a) Colburn j-factor, (b) friction factor and (c) modified volume goodness factor

CONCLUSION

Three-dimensional numerical simulations were performed of a compound heat exchanger consisting of louvered fins and delta winglet vortex generators. The delta winglets serve to reduce the size of the tube wakes, which are zones of poor heat transfer. The influence of the most important geometrical parameters on the thermal hydraulic performance of the compound heat exchanger was studied based on the Taguchi method. The delta winglets mainly contribute to the thermal and hydraulic performance at low Reynolds numbers. At higher Reynolds numbers the performance is mainly determined by the louvers. The compound heat exchanger has a better thermal hydraulic performance than when the louvers or the delta winglets are applied separately. The performance of the compound design is also compared to louvered, slit and plain fin heat exchangers. This clearly shows its potential. Especially for low Reynolds applications, the compound heat exchanger can be made smaller in size and thus more economical in cost (lower material and operational cost).

REFERENCES

[1] Achaichia A., and Cowell T.A., Heat transfer and pressure drop characteristics of flat tube and louvered plate fin surfaces, Experimental Thermal and Fluid Science, Vol. 1, 1988, pp. 147-157.

[2] Zhang X., and Tafti D.K., Flow efficiency in multi-louvered fins, International Journal of Heat and Mass Transfer, Vol. 46, 2003, pp. 1737–1750.

[3] DeJong N.C., and Jacobi A.M., Localized flow and heat transfer interactions in louvered fin arrays, International Journal of Heat and Mass Transfer, Vol. 46, 2003, pp. 443–455.

[4] Joardar A., and Jacobi A.M., A numerical study of flow and heat transfer enhancement using an array of delta-winglet vortex generators in a fin-and-tube heat exchanger, Journal of Heat Transfer, Vol. 129, 2007, pp. 1156-1167.

[5] Jacobi A.M., and Shah R.K., Heat transfer surface enhancement through the use of longitudinal vortices: A review of recent progress, Experimental Thermal and Fluid Science, Vol. 11(3), 1995, pp. 295-309.

[6] Torii K., Kwak K.M., Nishino K., Heat transfer enhancement accompanying pressure-loss reduction with winglet-type vortex generators for fin-tube heat exchangers, International Journal of Heat and Mass Transfer, Vol. 45(18), 2002, pp. 3795-3801.

[7] Bergles A.E., ExHFT for fourth generation heat transfer technology, Experimental Thermal and Fluid Science, Vol. 26, 2002, pp. 335-344.

[8] Tian L., He, Y., Tao Y., and Tao W., A comparative study on the air-side performance of wavy fin-and-tube heat exchanger with punched delta winglets in staggered and in-line arrangements, International Journal of Thermal Sciences, Vol. 48, 2009, pp. 1765-1776.

[9] Tian L., He Y., Chu P., and Tao W., Numerical study of flow and heat transfer enhancement by using delta winglets in a triangular wavy fin-and-tube heat exchanger, Journal of Heat Transfer, Vol. 131, 2009, paper number 091901 (8 pages).

[10] Ge H., Jacobi A.M., and Dutton J.C., Air-side heat transfer enhancement for offset-strip fin arrays using delta wing vortex generators, report ACRC, TR-205, Air Conditioning and Refrigeration Center, Urbana (IL), USA, 2002.
[11] Fan J.F., Ding W.K., Zhang J.F., He Y.L., and Tao W.Q., A performance evaluation plot of enhanced heat transfer techniques oriented for energy-saving, International Journal of Heat and Mass Transfer, Vol. 52, 2009, pp. 33-44.
[12] Joardar A., and Jacobi A.M., Impact of leading edge delta-wing vortex generators on the thermal performance of a flat tube, louvered-fin compact heat exchanger, International Journal of Heat and Mass Transfer, Vol. 48, 2005, pp. 1480-1493
[13] Lawson M.J., and Thole K.A., Heat transfer augmentation along the tube wall of a louvered fin heat exchanger using practical delta winglets, International Journal of Heat and Mass Transfer, Vol. 51, 2008, pp. 2346-2360.
[14] Huisseune H., T'Joen C., De Jaeger P., Ameel B., De Schampheleire S., and De Paepe M., Performance enhancement of a louvered fin heat exchanger by using delta winglet vortex generators, International Journal of Heat and Mass Transfer, 2012, under review.
[15] Soland J.G., Mack J.W.M., and Rohsenow W.M., Performance ranking of plate-fin heat exchanger surfaces, Journal of Heat Transfer - Transactions of the ASME, Vol. 100, 1978, pp. 514-519.
[16] Cui J., and Tafti D.K., Computations of flow and heat transfer in a three-dimensional multilouvered fin geometry, International Journal of Heat and Mass Transfer, Vol. 45(25), 2002, pp. 5007-5023.
[17] Tafti D.K., and Cui J., Fin-tube junction effects on flow and heat transfer in flat tube multilouvered heat exchangers, International Journal of Heat and Mass Transfer, Vol. 46(11), 2003, pp. 2027-2038.
[18] Jang J.Y., Wu M.C., and Chang W.J., Numerical and experimental studies of three-dimensional plate-fin and tube heat exchangers, International Journal of Heat and Mass Transfer, Vol. 39(14), 1996, pp. 3057-3066.
[19] Antoniou A.A., Heikal M.R., and Cowell T.A., Measurements of local velocity and turbulence levels in arrays of louvered plate fins, In: Proceedings of the 9th International Heat Transfer Conference, Jerusalem, Israel, 1990, pp. 105-110.
[20] Shah R.K., and Sekulic D.P., Fundamentals of Heat Exchanger Design, John Wiley & Sons, Inc., Hoboken, New Jersey, 2003.
[21] Schmidt T.E., Heat transfer calculation for extended surfaces, Refrigerating Engineering, Vol. 57, 1949, pp. 351-357.
[22] Wang C.C., Lee C.J., Chang C.T., and Lin S.P., Heat transfer and friction correlation for compact louvered fin-and-tube heat exchangers, International Journal of Heat and Mass Transfer, Vol. 42, 1999, pp. 1945-1956.
[23] Wu H.L., Gong Y., and Zhu X., Air flow and heat transfer in louver-fin round-tube heat exchangers, Journal of Heat Transfer, Vol. 129(2), 2007, pp. 200-210.
[24] Tang L.H., Zeng M., and Wang Q.W., Experimental and numerical investigation on air-side performance of fin-and-tube heat exchangers with various fin patterns, Experimental Thermal and Fluid Science, Vol. 33(5), 2009, pp. 818-827.
[25] Kays W.M., and London A.L., Compact Heat Exchangers, third ed., McGraw-Hill, New York, 1984.
[26] Huisseune H., Performance Evaluation of Louvered Fin Compact Heat Exchangers with Vortex Generators, Ph.D. dissertation, Ghent University, Belgium, 2011.
[27] Schmidt S.R. and Launsby R.G., Understanding industrial designed experiments, Air Academy Press, 1989, pp. 6.1-6.27.
[28] Qi Z.G., Chen J.P., Chen J., Parametric study on the performance of a heat exchanger with corrugated louvered fins, Applied Thermal Engineering, Vol. 27(2-3), 2007 pp. 539-544.
[29] Sahin B., A Taguchi approach for determination of optimum design parameters for a heat exchanger having circular-cross sectional pin fins, International Journal of Heat and Mass Transfer, Vol. 43, 2007, pp. 493-502.
[30] Zeng M., Tang L. H., Lin M., and Wang Q. W., Optimization of heat exchangers with vortex-generator fin by Taguchi method, Applied Thermal Engineering, Vol. 30(13), 2010, pp. 1775-1783.
[31] Lozza G., and Merlo U., An experimental investigation of heat transfer and friction losses of interrupted and wavy fins for fin-and-tube heat exchangers, International Journal of Refrigeration-Revue Internationale Du Froid, Vol. 24(5), 2001, pp. 409-416.
[32] Dong J.Q., Chen J.P., Chen Z.J., Zhang W.F., and Zhou Y.M., Heat transfer and pressure drop correlations for the multi-louvered fin compact heat exchangers, Energy Conversion and Management, Vol. 48(5), 2007, pp. 1506-1515.
[33] Pesteei S.M., Subbarao P.M.V., and Agarwal R.S., Experimental study of the effect of winglet location on heat transfer enhancement and pressure drop in fin-tube heat exchangers, Applied Thermal Engineering, Vol. 25, 2005, pp. 1684-1696.
[34] Sunden B., and Svantessen J., Correlation of j and f factors for multi-louvered heat transfer surfaces, Proceedings of third UK national heat transfer conference, United Kingdom, 1992, pp. 805-811.
[35] Fiebig M., Mitra N., and Dong Y., Simultaneous heat transfer enhancement and flow loss reduction of fin-tubes, Proceeding of Ninth International Heat Transfer Conference, Vol. 4, Jerusalem, 1990, pp. 51-55.
[36] Fan J.F., He Y.L., and Tao W.Q., Application of combined enhanced techniques for design of highly efficient air heat transfer surface, Proceedings of the 7th International Conference on Enhanced, Compact and Ultra-Compact Heat Exchangers: From Microscale Phenomena to Industrial Applications, Heredia, Costa Rica, ECI, 2009, pp. 87-96.
[37] Song G. D., and Nishino K., Numerical Investigation for Net Enhancement in Thermal-Hydraulic Performance of Compact Fin-Tube Heat Exchangers with Vortex Generators, Journal of Thermal Science and Technology, Vol. 3(2), 2008, pp. 368-380.
[38] Hwang S., and Jeong J.H., Flow field analysis of the air flowing through fin-and-tubes with delta-winglet vortex generator, Proceedings of the 7th International Conference on Enhanced, Compact and Ultra-Compact Heat Exchangers: From Microscale Phenomena to Industrial Applications, Heredia, Costa Rica, ECI, 2009, pp. 67-77.
[39] Fiebig M., Valencia A., and Mitra N.K., Wing-Type Vortex Generators for Fin-and-Tube Heat Exchangers, Experimental Thermal Fluid Science, Vol. 7, 1993, pp. 287-295.
[40] Bolboacua S.D., and Jäntschi L., Design of Experiments: useful orthogonal arrays for number of experiments from 4 to 16, Entropy, Vol. 9, 2007, pp. 198-232.
[41] Stone K.M., Review of Literature on Heat Transfer Enhancement in Compact Heat Exchangers, report ACRC, TR-105, Air Conditioning and Refrigeration Center, Urbana (IL), USA, 1996
[42] Wang C. C., Lee W. S., and Sheu W. J., A comparative study of compact enhanced fin-and-tube heat exchangers, International Journal of Heat and Mass Transfer, Vol. 44(18), 2001, pp. 3565–3573.
[43] Wang C. C., Chi K. Y., and Chang C. J., Heat transfer and friction characteristics of plain fin-and-tube heat exchangers, part II: Correlation, International Journal of Heat and Mass Transfer, Vol. 43(15), 2000, pp. 2693-2700.
[44] London A.L., and Ferguson C.K., Test results of high performance heat exchanger surfaces used in aircraft intercoolers and their significance for gas turbine regenerator design, Transactions of the ASME, 1949, pp. 17-26.
[45] Fujino H., Research and development on heat exchangers for air conditioners with alternative winglet, Proceedings of the 7th International Conference on Enhanced, Compact and Ultra-Compact Heat Exchangers: From Microscale Phenomena to Industrial Applications, Heredia, Costa Rica, ECI, 2009, pp. 201-207.